Structural and electronic properties of iron monoxide clusters Fe_nO and Fe_nO^- ($n=2-6$): A combined photoelectron spectroscopy and density functional theory study

Gennady L. Gutsev[a] and Charles W. Bauschlicher, Jr.
Mail Stop 230-3, NASA Ames Research Center, Moffett Field, California 94035

Hua-Jin Zhai and Lai-Sheng Wang[b]
Department of Physics, Washington State University, Richland, Washington 99352
and W. R. Wiley Environmental Molecular Sciences Laboratory, Pacific Northwest National Laboratory, Richland, Washington 99352

(Received 30 June 2003; accepted 4 September 2003)

We report a combined anion photoelectron spectroscopy and density functional theory (DFT) study on a series of iron monoxide clusters, Fe_nO ($n=2-6$). Well-resolved photoelectron spectra were obtained for Fe_nO^- at variable detachment energies, allowing the ground state and numerous low-lying excited states of Fe_nO to be observed. Sharp threshold photoelectron features were obtained for each species, which suggest rather small geometry changes between the anion and neutral ground states for the monoxide clusters and allows the electron affinities of the neutral clusters to be measured accurately. Extensive DFT calculations using the generalized gradient approximation were carried out for both Fe_nO and Fe_nO^-. Optimized geometries of the ground and lowest excited states of both the anion and neutral species are reported along with the ground-state vibrational frequencies and fragmentation energies. Theoretical electron affinities were compared with the experimental measurements to verify the ground states of the iron monoxide clusters obtained from the DFT calculations. © *2003 American Institute of Physics.*
[DOI: 10.1063/1.1621856]

I. INTRODUCTION

The interaction between iron and oxygen is relevant to understand important chemical and biochemical processes, such as corrosion and oxygen transport in biological systems. Iron monoxide clusters represent ideal model systems, which may help address these fundamental processes at the atomic level. However, the interaction of atomic oxygen with neutral and charged iron clusters is not yet well understood. Experimental spectroscopic data are known for the smallest FeO ($r_e=1.616$ Å,[1] $\omega_e=880\,\mathrm{cm}^{-1}$,[2] $\mu=4.17\pm0.08$ D,[3] $D_o=4.7\pm0.2$ eV[4]) and FeO^+ ($D_o=3.53\pm0.06$ eV[5]). For larger Fe_nO species, Fe_n^+-O binding energies were obtained from collision induced dissociation (CID) measurements[6] for $n=2-17$. Preliminary photodetachment photoelectron spectra of oxygen-chemisorbed iron cluster anions Fe_nO^- ($n=1-16$), as well as several O-rich iron clusters, were reported by one of us (L.S.W.).[7–10] Theoretical studies[11–14] have been performed for FeO and its ions at the *ab initio* and density functional theory (DFT) levels. For the larger species, the only computations that we are aware of are for the neutral Fe_nO ($n=2-6$) using DFT within a local spin density approximation (LSDA).[8]

The complicated electronic structure of transition metal systems, and iron clusters in particular, has posed considerable experimental and theoretical challenges. The aim of the present work is to obtain well-resolved photoelectron spectra of Fe_nO^- at various photon energies in order to better evaluate the electron affinities (EA), to resolve low-lying excited states of the corresponding neutral clusters, and to compare our experimental findings with the results of our extensive computations performed using density functional theory with the generalized gradient approximation (DFT-GGA). We also present optimized geometries of the ground- and lowest excited states of the Fe_nO and Fe_nO^- species ($n=2-6$), along with their ground-state vibrational frequencies and fragmentation energies. Such a combined experimental and computational study allows us to assign the ground states of the anionic and neutral iron monoxide clusters, which all have high spins. There are a large number of low-lying excited states for both the neutrals and anions.

II. EXPERIMENTAL AND COMPUTATIONAL DETAILS

A. Experimental methods

The experiments were carried out using a magnetic-bottle-type photoelectron spectroscopy (PES) apparatus equipped with a laser vaporization supersonic cluster source, details of which have been described previously.[15,16] Briefly, the Fe_nO^- cluster anions were produced by laser vaporization of a pure iron target in the presence of a helium carrier gas, and were analyzed using a time-of-flight mass spectrometer. The oxygen was either from residual oxygen in the source chamber/target surface or from N_2O (1%) seeded in the helium carrier gas. The Fe_nO^- ($n=2-6$) species were each mass selected and decelerated before being photodetached. Four detachment photon energies were used in the

[a]Electronic mail: ggutsev@mail.arc.nasa.gov
[b]Electronic mail: ls.wang@pnl.gov

 © 2003 American Institute of Physics

Downloaded 25 Mar 2007 to 130.20.226.164. Redistribution subject to AIP license or copyright, see http://jcp.aip.org/jcp/copyright.jsp

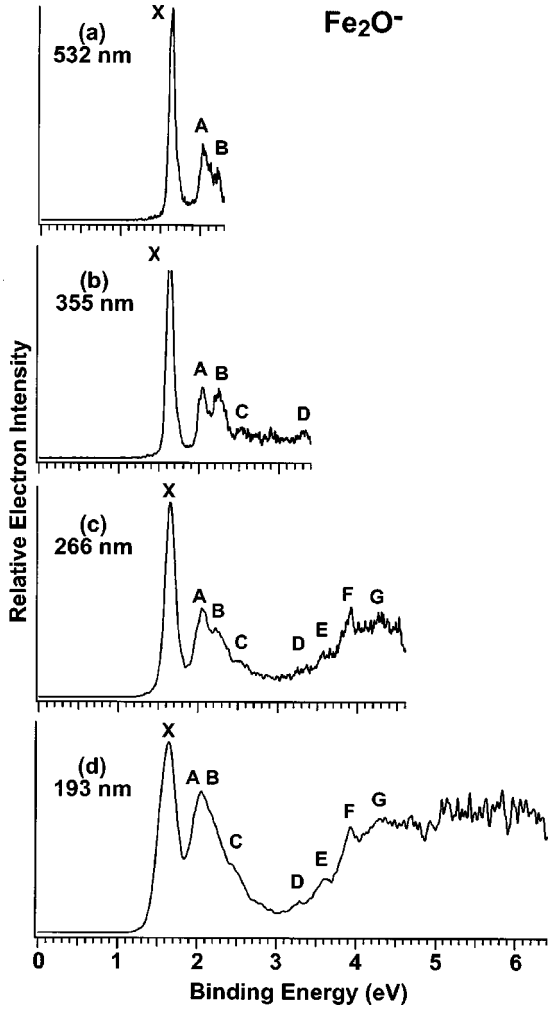

FIG. 1. Photoelectron spectra of Fe_2O^- at (a) 532 nm (2.331 eV); (b) 355 nm (3.496 eV); (c) 266 nm (4.661 eV); and (d) 193 nm (6.424 eV).

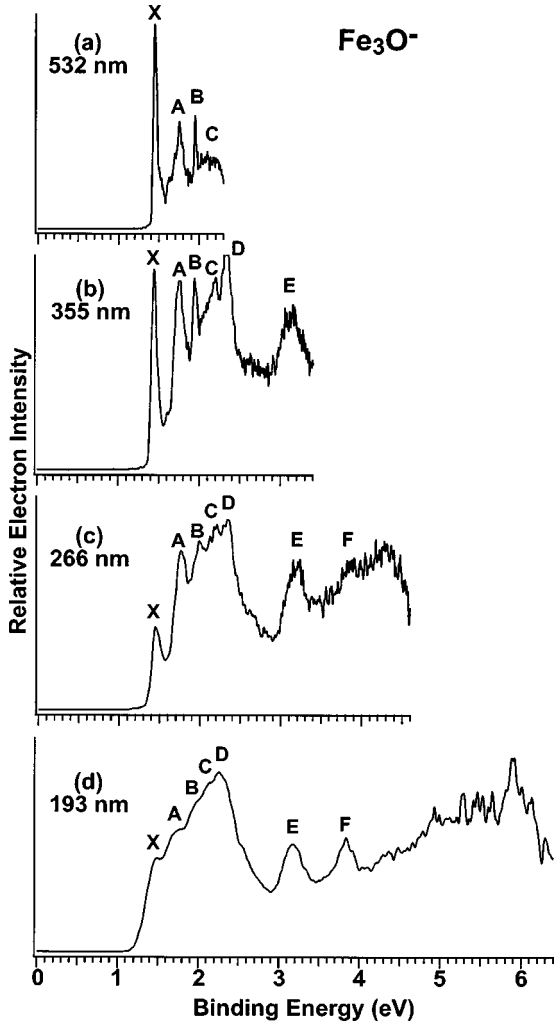

FIG. 2. Photoelectron spectra of Fe_3O^- at (a) 532 nm; (b) 355 nm; (c) 266 nm; and (d) 193 nm.

current study: 532 nm (2.331 eV), 355 nm (3.496 eV), 266 nm (4.661 eV), and 193 nm (6.424 eV). Photoelectrons were collected at nearly 100% efficiency by the magnetic bottle and analyzed in a 3.5 m long electron flight tube. The photoelectron spectra were calibrated using the known spectrum of Rh^-, and the energy resolution of the apparatus was $\Delta Ek/Ek \sim 2.5\%$, that is, ~25 meV for 1 eV electrons.

B. Theoretical procedures

The GAUSSIAN 98 program[17] was used for all the calculations. We used the basis sets denoted as 6-311+G* in the Gaussian program, namely $(15s11p6d1f)/[10s7p4d1f]$ for Fe (Refs. 18–20) and $(12s6p1d)/[5s4p1d]$ for O.[21] The following exchange-correlation functionals were tested on Fe_2O and Fe_2O^-: BLYP [Becke's exchange[22] and Lee–Yang–Parr's correlation[23]], BP86 [Becke's exchange[22] and Perdew's correlation[24]], BPW91 [Becke's exchange[22] and Perdew-Wang's correlation[25]], BPBE [Becke's exchange[22] and Perdew–Burke–Ernzerhof's correlation[26]], and hybrid B3LYP.[27,28] The BPW91 functional was used in the calculations for $n \geqslant 3$. Assignment of the spectroscopic states of Fe_2O and Fe_2O^- was based on the symmetry of the Slater determinants built using the one-electron DFT orbitals (hybrid or Kohn–Sham ones). Optimizations for $n \geqslant 3$ were performed without imposing symmetry constraints, and the optimized states are marked with the number of unpaired electrons $2S$, where S is the total spin.

The geometry of each species was optimized and a subsequent harmonic frequency calculation was performed using analytical second derivatives in order to confirm that the optimized geometry corresponded to a minimum. For the neutral species, the initial state had the same number of unpaired electrons as the corresponding bare Fe_n cluster.[29] States with fewer and greater numbers of open shells were studied until we were confident that we had found the ground state. The starting numbers of unpaired electrons of the Fe_nO^- anions were chosen as the numbers of unpaired electrons in the corresponding neutrals increased by 1, and then states with fewer and greater numbers of open shells were studied. Generally, three to five optimizations were performed in each case. Our reported electron affinities, EAs, are computed as the differences in total energies of each species at its equilibrium geometry, and therefore correspond to adiabatic values.

Downloaded 25 Mar 2007 to 130.20.226.164. Redistribution subject to AIP license or copyright, see http://jcp.aip.org/jcp/copyright.jsp

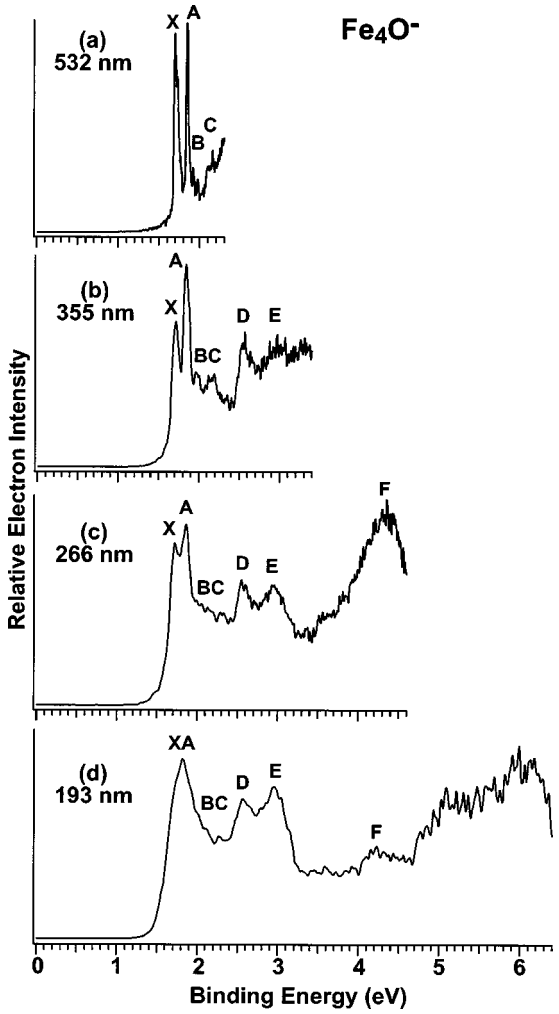

FIG. 3. Photoelectron spectra of Fe_4O^- at (a) 532 nm; (b) 355 nm; (c) 266 nm; and (d) 193 nm.

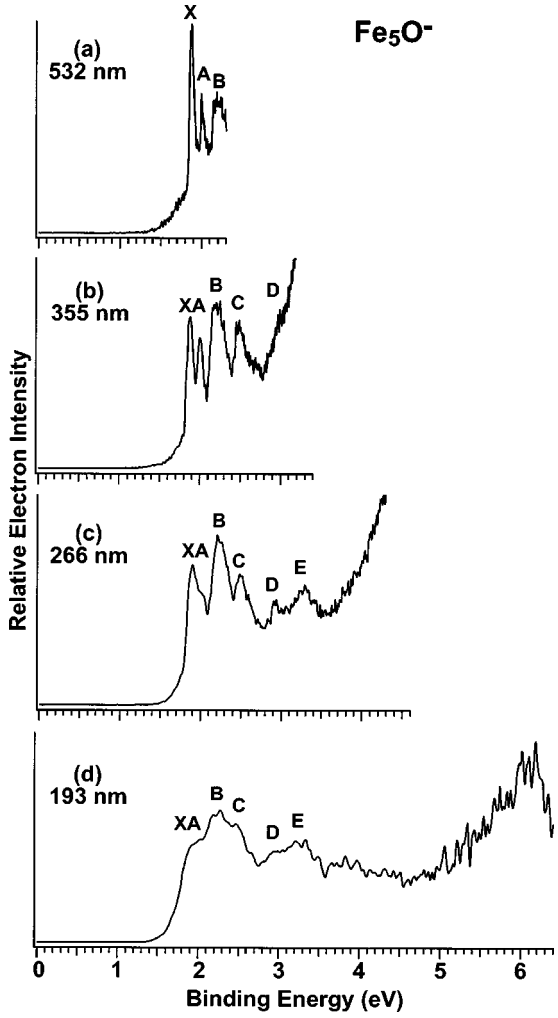

FIG. 4. Photoelectron spectra of Fe_5O^- at (a) 532 nm; (b) 355 nm; (c) 266 nm; and (d) 193 nm.

III. EXPERIMENTAL RESULTS

The photoelectron spectra for Fe_nO^- $(n=2-6)$ are shown in Figs. 1–5, respectively, at four photon energies: 532, 355, 266, and 193 nm. These data are significantly improved in comparison to our previous reports in several respects.[7,8,10] First, each species was studied at four different photon energies in the present work, whereas only the 355 and 266 nm photons were used previously. The low photon energy spectra at 532 nm allowed the low binding energy features to be better resolved, whereas the high photon energy spectra at 193 nm provide information about high-lying excited states of the neutral clusters. Second and more important, efforts were made to control the temperatures of the clusters by tuning the firing timing of the vaporization laser relative to the carrier gas, and choosing the later part of the cluster beam (where the clusters have a larger residence time in the nozzle and tend to be colder) for photodetachment.[30,31] The colder clusters give rise to sharper and better-resolved spectral features, which would have been smeared out otherwise even with good instrumental resolution.[32–34]

Numerous discrete and well-resolved electronic transitions were observed in the PES spectra of Fe_nO^- $(n=2-6)$, as shown in Figs. 1–5. The PES features represent the electronic transitions from the ground-state Fe_nO^- anions to the ground- and excited states of the corresponding Fe_nO neutrals. Basically, the lower binding energy portion (below ~2.5 eV) of the PES spectra for each Fe_nO^- species was better resolved with several well-separated sharp features. In particular, a sharp threshold peak was observed in each spectrum. Each feature is likely to represent a single electronic state of a neutral, which indicates that the energy levels near the Fermi level are not too congested. The narrow bandwidths of the low-energy peaks and the threshold peak, in particular, allows the suggestion that structural changes between the Fe_nO^- anions and their neutral counterparts are small. In contrast, the higher binding energy portion of the PES spectra for each Fe_nO^- species appeared to be extremely congested, and only few prominent features could be identified from the apparently continuous electron signals. The observed vertical detachment energies (VDE) for all the labeled features (X–F) in Figs. 1–5 are given in Table I.

We note that the temperature for the cluster anions was expected to be at around or slightly below room temperature[32] under our current experimental conditions. Consequently, hot band transitions were largely suppressed, as indicated by the disappearance or decrease of low binding

Downloaded 25 Mar 2007 to 130.20.226.164. Redistribution subject to AIP license or copyright, see http://jcp.aip.org/jcp/copyright.jsp

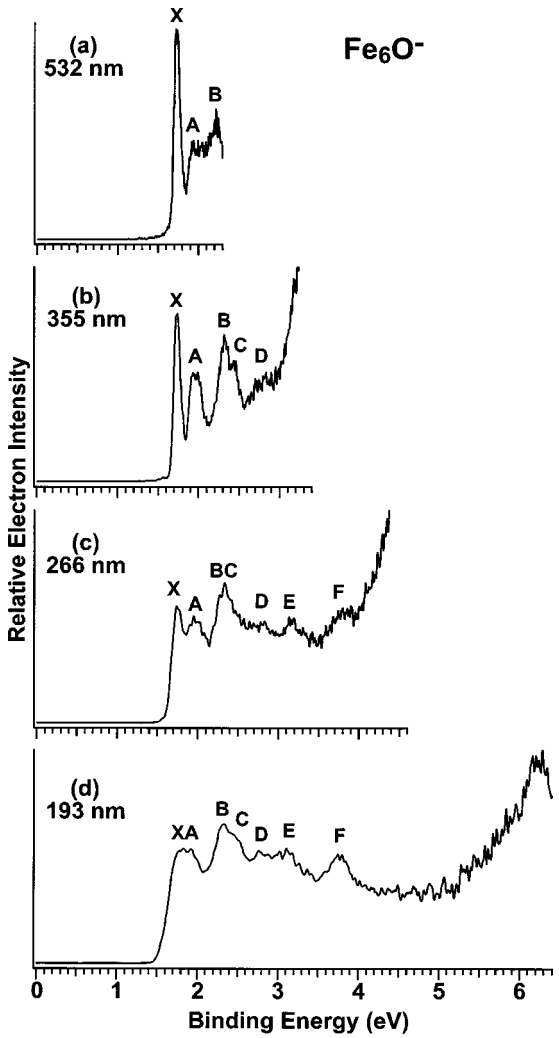

FIG. 5. Photoelectron spectra of Fe_6O^- at (a) 532 nm; (b) 355 nm; (c) 266 nm; and (d) 193 nm.

energy tails and the appearance of sharp onset of the threshold PES feature (X). Nevertheless, a substantial low binding energy tail was observed for the spectra of Fe_5O^- (Fig. 4), showing that the relatively large iron monoxide species were still hot under our current source conditions. Furthermore, the intense and increasing tails at the higher binding energy side of the PES spectra of Fe_5O^- and Fe_6O^- are characteristic of thermionic emission from hot clusters. The absence of such high binding energy tails in the spectra of Fe_2O^-, Fe_3O^-, and Fe_4O^- implies that these smaller monoxide species were relatively cold.

The well-resolved sharp threshold features (X) in Figs. 1–5 provide important information for the ground states of both the anions and the neutrals and facilitate comparison with the results of calculations. The sharp threshold peaks suggested that there is little geometry change between the ground states of the anions and the neutral clusters and that the extra electron in the anions occupies a nonbonding orbital. The peak maximum in each spectrum yielded the VDE for the ground-state transitions of Fe_nO^-, as listed in Table I. The sharp onset of the threshold peak (X) allowed a fairly accurate determination of the adiabatic detachment energies (ADE) for the ground-state transitions, i.e., the EAs of the corresponding Fe_nO neutral clusters. Since no vibrational structures were resolved, we evaluated the ADE by drawing a straight line at the leading edge of the feature X and then adding the instrumental resolution to the intersections with the binding energy axis. Although this is an approximate procedure, it yields consistent ADEs from spectra taken at different photon energies, due to the relative sharp onset of the spectra. All the ADEs were determined from the 532 nm spectra, which yielded the most accurate values because of a better spectral resolution. The ADEs obtained in this way are also given in Table I.

TABLE I. Adiabatic and vertical detachment energies (ADEs and VDEs) of Fe_nO^- derived from photoelectron spectra. All energies are in eV.

	Observed feature	ADE[a,b]	VDE[b]
Fe_2O^-	X	1.60(2)	1.64(2)
	A		2.04(2)
	B		2.25(2)
	C		2.52(5)
	D		3.30(5)
	E		3.60(5)
	F		3.92(5)
	G		~4.3
Fe_3O^-	X	1.44(2)	1.44(2)
	A		1.75(2)
	B		1.94(2)
	C		2.20(3)
	D		2.33(2)
	E		3.18(4)
	F		3.84(5)
Fe_4O^-	X	1.70(2)	1.70(2)
	A		1.85(2)
	B		1.97(3)
	C		2.16(5)
	D		2.56(3)
	E		2.95(5)
	F		~4.3
Fe_5O^-	X	1.85(2)	1.87(2)
	A		2.00(2)
	B		2.20(5)
	C		2.49(3)
	D		~2.9
	E		~3.3
Fe_6O^-	X	1.70(2)	1.73(2)
	A		1.96(3)
	B		2.32(3)
	C		2.43(3)
	D		~2.8
	E		~3.2
	F		3.78(6)

[a]Also represent the adiabatic electron affinities of the corresponding neutral Fe_nO species.
[b]Numbers in parentheses represent the experimental uncertainties in the last digit.

IV. THEORETICAL RESULTS

A. Structures and frequencies

In agreement with the previous discussion,[35] both Fe_2O and Fe_2O^- possess a number of closely spaced states for each spin multiplicity. We performed an extensive search within linear Fe–O–Fe, Fe–Fe–O, and angular symmetric and nonsymmetric Fe–O–Fe configurations. The ground

Downloaded 25 Mar 2007 to 130.20.226.164. Redistribution subject to AIP license or copyright, see http://jcp.aip.org/jcp/copyright.jsp

TABLE II. Results of computations on the ground states of Fe_2O ($^7A_2$) and Fe_2O^- ($^8A_2$) using different methods.

	B3LYP	BLYP	BPW91	BP86	BPBE
			$Fe_2O\ ^7A_2 \equiv {}^7A''$		
R_e(O–Fe), Å	1.799	1.804	1.789	1.787	1.789
∠FeOFe°	70.64	71.70	71.58	71.55	71.55
$\omega\,(b_2)$, cm^{-1}	224	268	286	287	287
$\omega\,(a_1)$	351	329	343	343	343
$\omega\,(a_1)$	731	715	730	734	730
μ, Debye	3.199	2.862	2.805	2.780	2.800
EA, eV[a]	1.39	1.21	1.30	1.44	1.28
			$Fe_2O^-\ ^8A_2 \equiv {}^8A''$		
R_e(O–Fe), Å	1.848	1.849	1.833	1.831	1.832
∠FeOFe°	68.4	69.76	69.50	69.53	69.53
$\omega\,(b_2)$, cm^{-1}	144	266	273	281	274
$\omega\,(a_1)$	330	302	317	315	317
$\omega\,(a_1)$	666	647	667	670	668

[a]Experimental value (this work) is 1.60±0.02 eV.

states of Fe_2O and Fe_2O^- were found to be $^7A_2$ and $^8A_2$, respectively. We should note that the $^7A_1$ state of Fe_2O has essentially the same geometry as the ground $^7A_2$ state, and is computed to be only 0.06 eV above. Thus, we cannot rule out the $^7A_1$ as the ground state of Fe_2O. However, the $^7A_1$ state is not related to the $^8A_2$ state of the anion by a one-electron detachment process, and therefore would not be observed in the experiment. The Mulliken populations show that the charge on the oxygen increases from $-0.39e^-$ in Fe_2O to $-0.54e^-$ in Fe_2O^-. That is, the extra electron adds mostly into the Fe 4*s* orbitals, which were depleted by donation to the oxygen in the neutral clusters.

Optimizations performed without imposing C_{2v} symmetry constraints yielded $^7A''$ and $^8A''$ states with identical total energies and bond lengths as those for the $^7A_2$ and $^8A_2$ states, respectively. As shown in Table II, all five methods tested provide similar geometrical structures and vibrational frequencies except for the B3LYP, which predicts the bending frequency of the Fe_2O^- anion to be too low. All the EAs computed at the different levels of theory are smaller than the experimental value, with the largest deviation (~0.4 eV) seen at the BLYP level (Table II). The Perdew's correlation functionals PW91, P86, and PBE provide nearly identical geometries and vibrational frequencies. The best EA with respect to the experiment was obtained at the BP86 level. However, this method overestimated the EAs of pure iron clusters.[29]

The structures of Fe_2O and Fe_2O^- with different spin multiplicities were optimized at the BPW91 level and are presented in Fig. 6. One can see a rather striking peculiarity: the ferromagnetic high-spin ground states are very close in total energy to the low-spin antiferromagnetic states. The latter possesses two nonequivalent Fe atoms. By imposing C_{2v} symmetry constraints, one can obtain a nonmagnetic singlet of Fe_2O, but this nonmagnetic $^1A_1$ state [r_e(O–Fe) = 1.69 Å, r_e(Fe–Fe) = 2.12 Å] is 2.27 eV above the antifer-

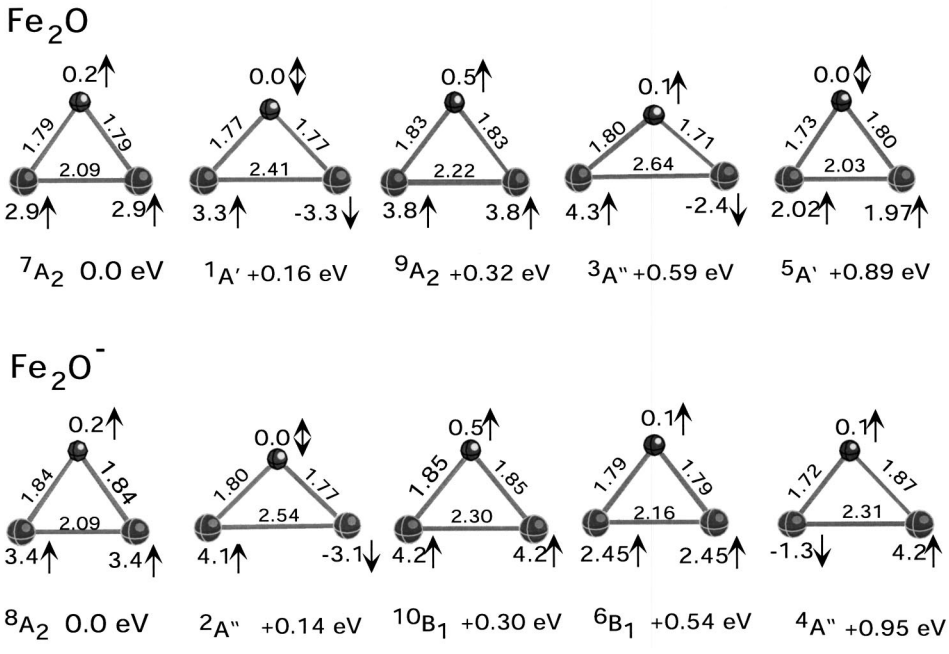

FIG. 6. Lowest energy states of Fe_2O and Fe_2O^-. Bond lengths are in Å and local magnetic moments in bold at each atom are in bohr magnetons. Total energies of the corresponding ground states are taken as zero for both series.

Downloaded 25 Mar 2007 to 130.20.226.164. Redistribution subject to AIP license or copyright, see http://jcp.aip.org/jcp/copyright.jsp

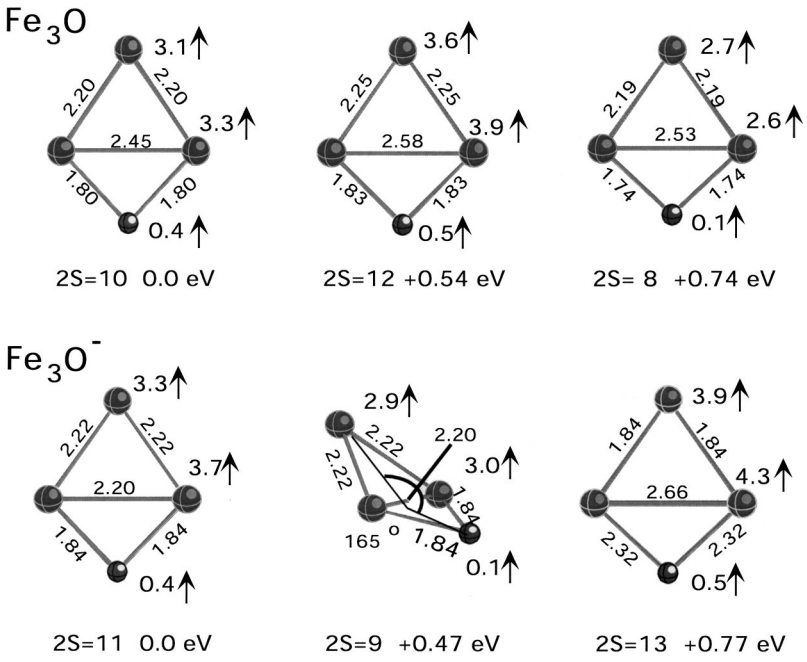

FIG. 7. Lowest energy states of Fe_3O and Fe_3O^-. See the caption of Fig. 6. The total numbers of unpaired electrons are labeled as $2S$.

romagnetic $^1A'$ state. For the doublet Fe_2O^- anion, imposing C_{2v} constraints leads to a state that is unbound.

Figures 7–10 display optimized ground-state structures of neutral Fe_nO $(n=3-6)$ and their anions, along with the low-lying states possessing the number of unpaired electrons adjacent to those in the corresponding ground states. Oxygen is twofold coordinated in species with $n=3$ and 4, while it is threefold coordinated in the larger clusters. This is in agreement with the previous LSDA results,[8] except that the latter predicted that a twofold (edge-on) oxygen adsorption is more stable for Fe_5O. We found the lowest energy edge-on structure for Fe_6O^- to correspond to a $2S=17$ state, which is above the $2S=19$ ground state (Fig. 10) by 0.29 eV.

Small iron clusters are highly magnetic with numerous unpaired electrons. Excluding Fe_4O, the number of unpaired electrons in ground states of Fe_n and Fe_nO are the same. The

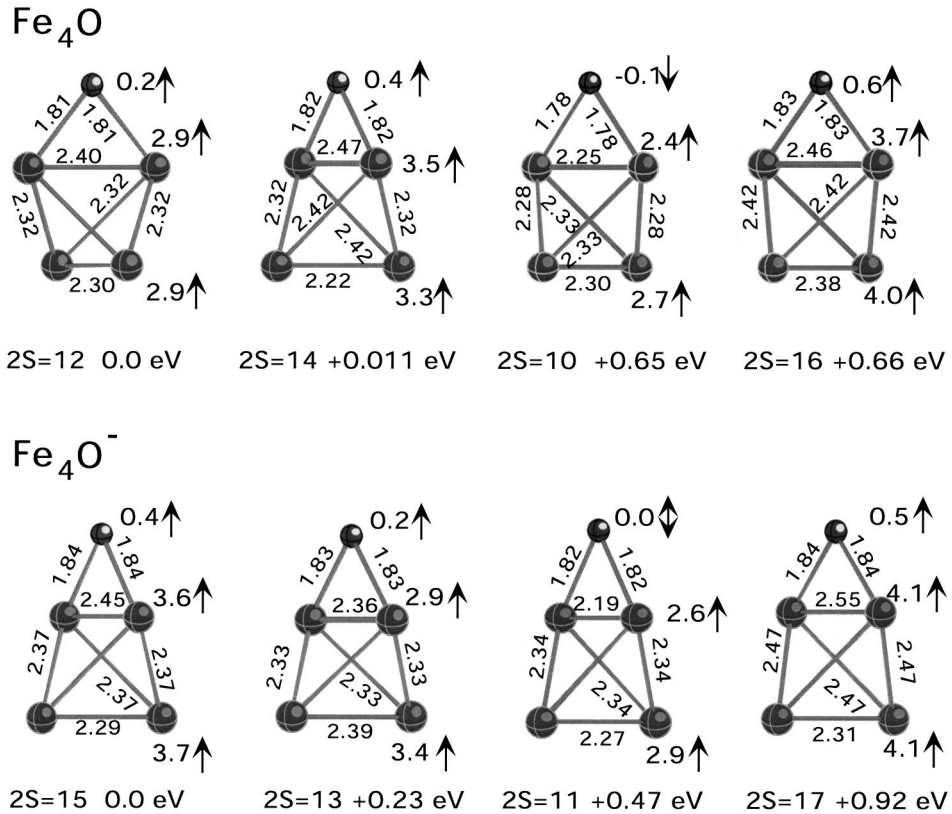

FIG. 8. Lowest energy states of Fe_4O and Fe_4O^-. See the captions in Figs. 6 and 7.

Downloaded 25 Mar 2007 to 130.20.226.164. Redistribution subject to AIP license or copyright, see http://jcp.aip.org/jcp/copyright.jsp

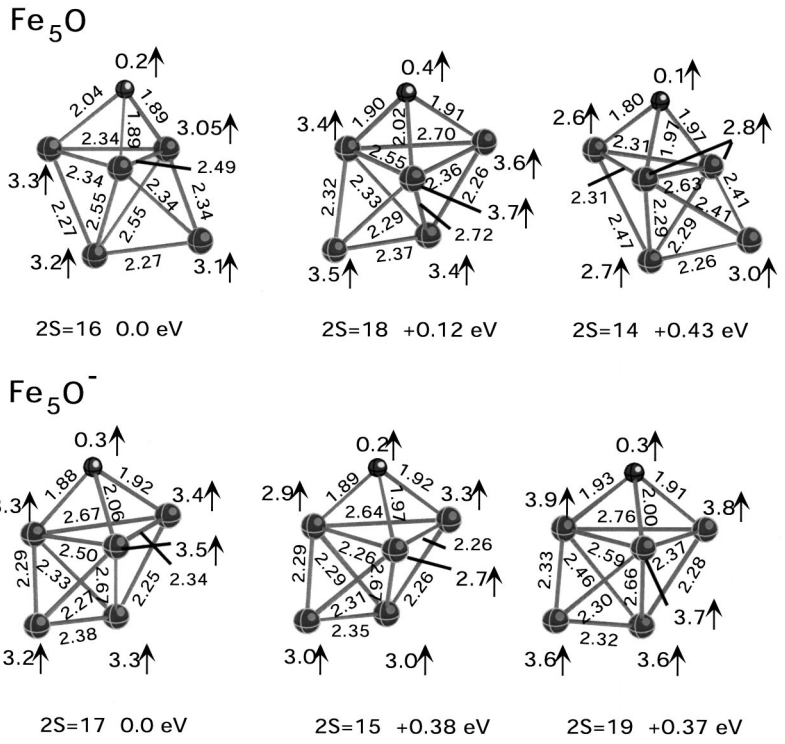

FIG. 9. Lowest energy states of Fe_5O and Fe_5O^-. See the captions in Figs. 6 and 7.

difference between the total energies of the Fe_4O states with $2S=12$ and $2S=14$ is only 0.011 eV, which seems to be related to a small separation between the $2S=12$ and $2S=14$ states of bare Fe_4 (its $2S=14$ state is lower by 0.08 eV as computed[29] at the same BPW91/6-311+G* level). (Salahub and Chrétien[36] found a higher separation of 0.36 eV at the PP86 level.) Thus, oxidation of the iron clusters, at least in the range of $2 \leqslant nZ \leqslant 6$ considered here at the BPW91/6-311+G* level of theory, appears not to quench the magnetic moments of the bare iron clusters.

Excluding Fe_4O, the number of unpaired electrons in the anion ground states differs by only 1 with respect to the number of unpaired electrons in the ground state of the corresponding neutrals. The ground state of Fe_4O^- has $2S=15$ and is well separated from the states with $2S=13$ and $2S=17$ (Fig. 8), while the neutral state of Fe_4O with

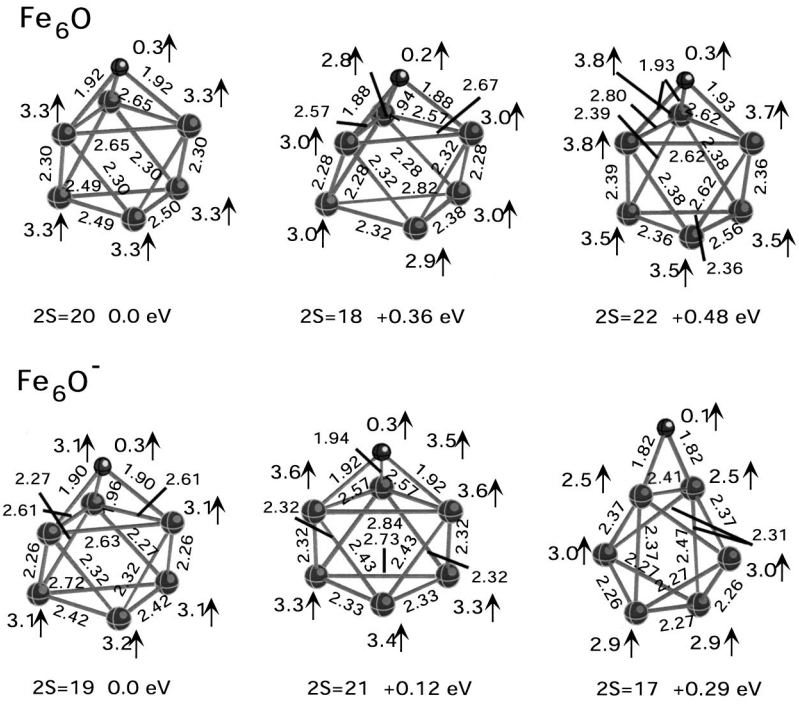

FIG. 10. Lowest energy states of Fe_6O and Fe_6O^-. See the captions in Figs. 6 and 7.

Downloaded 25 Mar 2007 to 130.20.226.164. Redistribution subject to AIP license or copyright, see http://jcp.aip.org/jcp/copyright.jsp

TABLE III. BPW91 harmonic vibrational frequencies (in cm^{-1}) and relative intensities of Fe_3O, Fe_4O, Fe_5O, Fe_6O, and their anions. Absolute intensities [KM/Mole]: Fe_3O:68.8, Fe_4O:90.3, Fe_5O:64.2, Fe_6O:57.7; Fe_3O^-:107.6, Fe_4O^-:126.6, Fe_5O^-:62.5, Fe_6O^-:56.9.

Freq.	Fe_3O	Fe_3O^-	Fe_4O	Fe_4O^-	Fe_5O	Fe_5O^-	Fe_6O	Fe_6O^-
ω_1	115[0.14]	143[0.01]	108[0.01]	99[0.04]	95[0.01]	105[0.01]	106[0.00]	105[0.01]
ω_2	220[0.03]	221[0.00]	115[0.01]	161[0.00]	102[0.01]	143[0.01]	112[0.00]	114[0.00]
ω_3	232[0.37]	230[0.24]	174[0.01]	167[0.00]	156[0.02]	159[0.00]	153[0.00]	138[0.00]
ω_4	336[0.00]	347[0.00]	191[0.02]	202[0.00]	165[0.02]	173[0.02]	153[0.00]	139[0.00]
ω_5	489[0.17]	406[0.37]	235[0.02]	231[0.04]	180[0.02]	185[0.03]	172[0.00]	171[0.01]
ω_6	650[1.00]	613[1.00]	238[0.01]	233[0.02]	207[0.03]	208[0.02]	185[0.01]	193[0.00]
ω_7			353[0.00]	343[0.00]	212[0.09]	227[0.00]	222[0.00]	206[0.00]
ω_8			431[0.00]	382[0.11]	235[0.19]	244[0.07]	222[0.00]	217[0.00]
ω_9			639[1.00]	612[1.00]	297[0.01]	285[0.02]	231[0.05]	235[0.01]
ω_{10}					326[0.02]	334[0.01]	285[0.08]	280[0.00]
ω_{11}					372[0.16]	380[0.10]	285[0.08]	299[0.01]
ω_{12}					562[1.00]	537[1.00]	330[0.00]	321[0.04]
ω_{13}							349[0.01]	335[0.01]
ω_{14}							352[0.01]	372[0.00]
ω_{15}							531[1.00]	524[1.00]

$2S=14$ is slightly above the state with $2S=12$. Since the anion and neutral tend to differ by only one unpaired electron, we would not be surprised if the ground state of Fe_4O is in fact a $2S=14$ state if a higher-level theory is applied.

Harmonic vibrational frequencies for the ground states of Fe_nO and Fe_nO^- are presented in Table III. The highest frequency mode is associated with the Fe_n-O stretching. The Fe_n-O bending modes depend on the shape of the corresponding metal cluster. For example, the second highest frequency mode in Fe_4O corresponds to the vibration of the O parallel to the upper two Fe atoms, while the lowest frequency mode is the vibration of the O perpendicular to the

TABLE IV. Fragmentation energies (in eV) of neutral and negatively charged iron monoxide clusters.

Neutral		Anion	
Channel	BPW91	Channel	BPW91
$Fe_2O \rightarrow Fe_2+O$	5.62	$Fe_2O^- \rightarrow Fe_2^-+O$	5.96
$\rightarrow FeO+Fe$	2.60	$Fe_2O^- \rightarrow Fe_2+O^-$	5.31
		$Fe_2O^- \rightarrow FeO^-+Fe$	2.62
$Fe_3 \rightarrow Fe_2+Fe$[a]	*2.32* (**1.91**)	$Fe_3^- \rightarrow Fe_2^-+Fe$	*2.84*
$Fe_3O \rightarrow Fe_3+O$	6.29	$Fe_3O^- \rightarrow Fe_3^-+O$	6.17
$\rightarrow Fe_2O+Fe$	2.99	$\rightarrow Fe_2O^-+Fe$	3.05
$\rightarrow FeO+Fe_2$	3.40	$\rightarrow FeO^-+Fe_2$	3.47
		$\rightarrow FeO+Fe_2^-$	3.78
$Fe_4 \rightarrow Fe_3+Fe$[a]	*3.06* (**2.19**)	$Fe_4^- \rightarrow Fe_3^-+Fe$	*3.34*
$Fe_4O \rightarrow Fe_4+O$	6.01	$Fe_4O^- \rightarrow Fe_4^-+O$	5.84
$\rightarrow Fe_3O+Fe$	2.70	$\rightarrow Fe_3O^-+Fe$	3.01
$\rightarrow Fe_2O+Fe_2$	3.56	$\rightarrow Fe_2O^-+Fe_2$	3.86
$\rightarrow FeO+Fe_3$	3.82	$\rightarrow FeO^-+Fe_3$	4.16
$Fe_5 \rightarrow Fe_4+Fe$[a]	*3.26* (**2.25**)	$Fe_5^- \rightarrow Fe_4^-+Fe$	*3.37*
$Fe_5O \rightarrow Fe_5+O$	5.80	$Fe_5O^- \rightarrow Fe_5^-+O$	5.59
$\rightarrow Fe_4O+Fe$	3.09	$\rightarrow Fe_4O^-+Fe$	3.12
$\rightarrow Fe_3O+Fe_2$	3.66	$\rightarrow Fe_3O^-+Fe_2$	3.97
$\rightarrow Fe_2O+Fe_3$	4.33	$\rightarrow Fe_2O^-+Fe_3$	4.67
$\rightarrow FeO+Fe_4$	3.88	$\rightarrow FeO^-+Fe_4$	4.28
		$\rightarrow Fe_5+O^-$	5.80
$Fe_6 \rightarrow Fe_5+Fe$[a]	*3.74* (**3.17**)	$Fe_6^- \rightarrow Fe_5^-+Fe$	*3.51*
$Fe_6O \rightarrow Fe_6+O$	5.70	$Fe_6O^- \rightarrow Fe_6^-+O$	5.67
$\rightarrow Fe_5O+Fe$	3.64	$\rightarrow Fe_5O^-+Fe$	3.54
$\rightarrow Fe_4O+Fe_2$	4.54	$\rightarrow Fe_4O^-+Fe_2$	4.47
$\rightarrow Fe_3O+Fe_3$	4.98	$\rightarrow Fe_3O^-+Fe_3$	5.17
$\rightarrow Fe_2O+Fe_4$	4.93	$\rightarrow Fe_2O^-+Fe_4$	5.18
$\rightarrow FeO+Fe_5$	4.21	$\rightarrow FeO^-+Fe_5$	4.50
		$\rightarrow Fe_6+O^-$	5.59
$Fe_7 \rightarrow Fe_6+Fe$[b]	3.11		

[a]Bond strengths of pure iron clusters: BPW91 values (in *italic*) are from Ref. 29, experimental data (in **bold**) are from Ref. 6.

[b]Experimental data from Ref. 6.

Downloaded 25 Mar 2007 to 130.20.226.164. Redistribution subject to AIP license or copyright, see http://jcp.aip.org/jcp/copyright.jsp

TABLE V. Experimental and BPW91 adiabatic electron affinities (EA, in eV) of bare iron clusters and iron monoxide clusters along with the BPW91 vertical detachment energies (VDE, in eV) from the Fe_nO^- ground states to the low and high spin states of the corresponding neutrals.

		Fe	Fe_2	Fe_3	Fe_4	Fe_5	Fe_6
EA	BPW91[a]	0.63	0.94	1.47	1.76	1.84	1.61
	Expt.[b]	0.151±0.003	0.902±0.008	1.45±0.08	1.80±0.05	1.75±0.05	1.61±0.05
		FeO	Fe_2O	Fe_3O	Fe_4O	Fe_5O	Fe_6O
EA	BPW91[c]	1.26	1.30	1.34	1.60	1.63	1.53
	Expt.[d]	1.50±0.02	1.60±0.02	1.44±0.02	1.70±0.02	1.85±0.02	1.70±0.02
		FeO	Fe_2O	Fe_3O	Fe_4O	Fe_5O	Fe_6O
VDE	Low spin	2.45	1.32	1.36	1.67	1.68	1.93
	High spin	1.26	1.68	1.91	2.30	1.77	1.65
	Expt.	1.50±0.02	1.64±0.02	1.44±0.02	1.70±0.02	1.87±0.02	1.73±0.02

[a]See Ref. 29.
[b]The EA of Fe and the EA of Fe_2 are from Ref. 41. The rest are unpublished data from the Wang group, which are slightly improved over those in Ref. 33.
[c]This work, the EA of FeO is from Ref. 13.
[d]This work (the PES data for FeO^- not shown). The EA of FeO obtained by Engelking and Lineberger (Ref. 40) is 1.492±0.020 eV.

upper two Fe atoms. For Fe_6O, the oxygen interacts with three Fe atoms, and the bending frequencies corresponds to the second and third highest frequency modes. Compared to the vibrational frequencies of the bare iron clusters,[29] they are generally larger. For example, the vibrational frequencies of Fe_3 are 62, 231, and 353 cm^{-1}, while Fe_3O has the lowest and highest frequencies of 115 and 650 cm^{-1}, respectively. While not relevant to the photodetachment experiment, we also report the infrared intensities to aid the interpretation of any future matrix experiments. The infrared intensities of the iron monoxide clusters are larger than those of bare iron clusters. For each molecule, most of the intensity falls into the highest frequency mode.

B. Thermodynamic stability

Fragmentation energies for different channels of the neutral and charged Fe_nO species were computed as differences in total energies of a species and its decay products corrected for the ZPEs, as presented in Table IV. For comparison, we included the Fe-abstraction energies from the bare iron clusters that were previously computed[29] and were also obtained[6] from the CID measurements. The Fe_n-O binding energies were found to be much higher than the $Fe_{n-1}-Fe$ energies. A comparison of the computed and experimental $Fe_{n-1}-Fe$ bond strengths shows that the BPW91 approach, as well as other pure DFT methods, tends to overestimate the bond strengths by about 1 eV. For comparison, the bond strength in the ground-state O_2 dimer computed at the same BPW91/6-311+G* level is 5.72 eV; the experimental value[37] is 5.12 eV. The bonding of the O atom to iron clusters is of a similar strength and is nearly independent of the cluster size. The charged Fe_nO^- clusters also possess high $Fe_n^- - O$ binding energies, owing to similar EAs of the Fe_n and Fe_nO clusters, as will be discussed below.

V. COMPARISON OF EXPERIMENTAL AND THEORETICAL RESULTS

The three lowest states of Fe_2O that are connected to the ground $^8A_2$ state of the anion are the $^7A_2$ ground state and the $^9A_2$ and $^7B_1$ excited states, which are 0.32 and 0.78 eV above the $^7A_2$ state, respectively. Detachment to form the $^7A_2$ state is associated with the peak labeled X in Table I and Fig. 1. On the basis of our computed excitation energies, the $^9A_2$ state probably corresponds to peak A, while the formation of the $^7B_1$ state is associated with either B or C. We performed a Franck–Condon analysis[38,39] for the $^7A_2$, $^9A_2$, and $^7B_1$ states, and the shape and width of the primary detachment peak are similar for all three states. This is different from what is observed in experiment. Thus, the intensity of the peaks is likely due to the character of the orbital from which the electron is detached. For all of the systems, the highest occupied α spin orbital of the anion is mostly of Fe $4s$ character, while the highest occupied β spin orbital is a mixture of Fe $4s$ and $3d$. There is only a small oxygen component in either the highest occupied α or β orbital. The other open-shell α orbitals tend to have a smaller $4s$ component than the highest occupied α orbital, but a bigger $4s$ component than the highest occupied β orbital. Because $4s$ detachments have larger cross sections than $3d$ detachments, we expect that detaching an α electron to form the low-spin neutral should have a larger intensity than detaching a β electron to form the high-spin neutral. For all systems the X peak is one of the most intense at the lowest detachment energy (532 nm), consistent with detachment from an orbital with the mostly Fe $4s$ character and rather similar geometries for the neutral and its anion. While this is consistent with the BPW91 results for Fe_2O^- to Fe_5O^-, the calculations predict a detachment of a β electron for Fe_6O^-. However, the $2S=19$ and 21 states of Fe_6O^- and the $2S=20$ and 18 states of Fe_6O are close in energy, and therefore it is possible that the ordering of the low-lying states of either the anion or neutral is incorrect.

Experimental and theoretical EAs of the Fe_nO clusters are compared in Table V and Fig. 11. We also include results for FeO, and we note that our experimental value is very close to that of Engelking and Lineberger.[40] For comparison, we also give experimental[33,41] and theoretical[29] EAs of the bare Fe_n clusters. Three observations can be made immediately. First, the difference between the adiabatic and vertical detachment energies is small in both theory and experiment. Second, the size-dependent trend in Fe_nO is reasonably re-

Downloaded 25 Mar 2007 to 130.20.226.164. Redistribution subject to AIP license or copyright, see http://jcp.aip.org/jcp/copyright.jsp

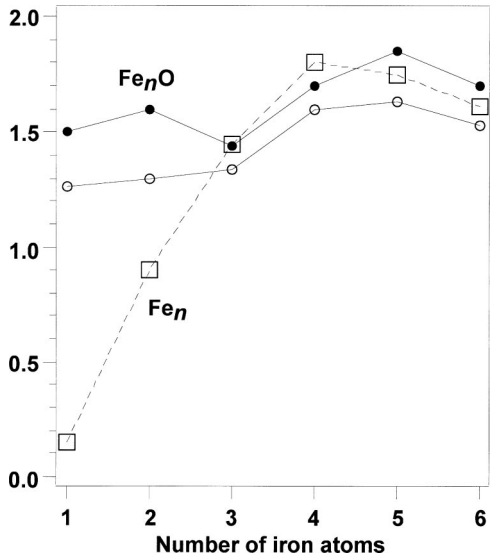

FIG. 11. Comparison of the experimental (filled dots) and BPW91 (empty dots) adiabatic electron affinities (in eV) of Fe_nO obtained in the present work with previous experimental (empty squares) data for the bare Fe_n clusters.

produced by the BPW91. Third, upon oxidation by the atomic oxygen, the EAs increase markedly only for the smallest species ($n=1$ and 2), whereas for larger species ($n=3-6$) oxidation only slightly changes the EAs. The EA trend of Fe_nO vs Fe_n may be understood from the anion-to-neutral structural changes of the iron monoxide. As can be seen in Figs. 7–10, for the $n=3-6$ monoxides, the major structural changes between the anions and neutrals take place in the Fe–Fe bond lengths, whereas the Fe–O bond lengths change very little. This is consistent with the metal-based nature of the anion HOMOs and explains why the oxidization of atomic oxygen does not lead to appreciable increase of the EAs for these relatively large monoxide species (Fig. 11). On the other hand, photodetachment from Fe_2O^- induces primarily changes in the Fe–O bond length without substantial change of the Fe–Fe bond length. An inspection of the anion HOMO shows that it is antibonding between oxygen and the Fe atoms, and weakly bonding between the two Fe atoms. That is why oxidation of Fe_2 leads to an apparent increase in the EA (Fe_2O vs Fe_2, Fig. 11).

It should be pointed out that while the theoretical EAs agree well with the experimental data for the bare Fe_2-Fe_6 clusters, the EAs are less accurately reproduced for the monoxide species Fe_nO ($n=2-6$). The BPW91 method underestimates the EAs by 0.1–0.2 eV for most monoxide species; the largest difference between theory and experiment reaches 0.30 eV for Fe_2O. Increasing the basis set for oxygen to 6-311++G($3df$) did not result in any appreciable change in the EA of Fe_2O. However, such discrepancies are still within the typical error bars of the DFT methods and are acceptable. For the atomic EA, the overestimation is probably related to an incorrect description of the ground-state $4s^2 3d^6$ configuration of the Fe atom, where the pure DFT methods are biased[42] toward a mixed $4s^{2-\delta}3d^{6+\delta}$ occupation.

Good agreement between our theoretical and experimental EAs lends credence to the current DFT calculations of both the monoxide anions and the neutrals. It is safe, in general, to assign the threshold PES feature (X) in Figs. 1–5 to the transition from the anion ground state to the neutral ground state identified in the DFT calculations (Figs. 6–10), respectively. These ground-state transitions are well characterized by one-electron detachment processes, as indicated by the spin states. Therefore, we would not be surprised to find that the true ground state of Fe_4O is the $2S=14$ state (Fig. 8), even though it is computed to be slightly higher in energy (by 0.011 eV) than the $2S=12$ state, because the ground state of Fe_4O^- is clearly the state with $2S=15$.

VI. SUMMARY

In summary, we report a combined anion photoelectron spectroscopy and density functional theory study on a series of iron monoxide clusters, Fe_nO ($n=2-6$). Well-resolved photoelectron spectra were obtained for Fe_nO^- at several photon energies, allowing the ground- and numerous low-lying excited states of Fe_nO to be observed. The ground-state adiabatic and vertical detachment energies were determined more accurately from the well-resolved spectra obtained at low photon energies. Sharp threshold features were observed for all the Fe_nO^- species, which indicates rather small geometry changes between the monoxide anions and the corresponding neutrals upon photodetachment. Extensive density functional theory calculations with generalized gradient approximation were carried out for both Fe_nO and Fe_nO^- with different spin states. Optimized geometries of the ground- and lowest excited states of both anion and neutral species are reported, along with their ground-state vibrational frequencies and fragmentation energies. Theoretical adiabatic detachment energies are compared with the experimental measurements, and good agreement is achieved.

ACKNOWLEDGMENTS

The theoretical work done in California was supported from NASA Ames Research Center through Contract NAS2-99092 to Eloret Corporation to G.L.G. The experimental work done in Washington was supported by the National Science Foundation (CHE-9817811) and was performed at the W. R. Wiley Environmental Molecular Sciences Laboratory, a national scientific user facility sponsored by DOE's Office of Biological and Environmental Research and located at the Pacific Northwest National Laboratory, operated for DOE by Battelle. The Franck–Condon simulations were performed using FCFGAUS, and these authors would like to thank K. M. Ervin for making this program available to them.

[1] A. S. C. Cheung, N. Lee, A. M. Lyyra, and A. J. Merer, J. Mol. Spectrosc. **95**, 213 (1982).
[2] D. W. Green, G. T. Reedy, and J. G. Kay, J. Mol. Spectrosc. **78**, 257 (1979).
[3] T. C. Steimle, D. F. Nachman, J. E. Shirley, and A. J. Merer, J. Chem. Phys. **90**, 5360 (1989).
[4] A. J. Merer, Annu. Rev. Phys. Chem. **40**, 407 (1989).
[5] E. R. Fisher, J. L. Elkind, D. E. Clemmer, R. Georgiadis, S. K. Loh, N. Aristov, L. S. Sunderlin, and P. B. Armentrout, J. Chem. Phys. **93**, 2676 (1990).

Downloaded 25 Mar 2007 to 130.20.226.164. Redistribution subject to AIP license or copyright, see http://jcp.aip.org/jcp/copyright.jsp

[6] P. B. Armentrout, Annu. Rev. Phys. Chem. **52**, 423 (2001).
[7] L. S. Wang, H. Wu, and S. R. Desai, Phys. Rev. Lett. **76**, 4853 (1996).
[8] L. S. Wang, J. Fan, and L. Lou, Surf. Rev. Lett. **3**, 695 (1996).
[9] J. Fan and L. S. Wang, J. Chem. Phys. **102**, 8714 (1995).
[10] H. Wu, S. R. Desai, and L. S. Wang, J. Am. Chem. Soc. **118**, 5296 (1996).
[11] C. W. Bauschlicher, Jr. and P. Maitre, Theor. Chim. Acta **90**, 189 (1995).
[12] J. F. Harrison, Chem. Rev. (Washington, D.C.) **100**, 679 (2000).
[13] G. L. Gutsev, B. K. Rao, and P. Jena, J. Phys. Chem. A **104**, 5374 (2000).
[14] Y. Nakao, K. Hirao, and T. Taketsugu, J. Chem. Phys. **114**, 7935 (2001).
[15] L. S. Wang, H. S. Cheng, and J. Fan, J. Chem. Phys. **102**, 9480 (1995).
[16] L. S. Wang and H. Wu, in *Advances in Metal and Semiconductor Clusters, Vol. 4, Cluster Materials*, edited by M. A. Duncan (JAI, Greenwich, 1998), pp. 299–343.
[17] M. J. Frisch, G. W. Trucks, H. B. Schlegel *et al.*, GAUSSIAN 98, Revision A.11, Gaussian, Inc., Pittsburgh, PA, 2001.
[18] A. J. H. Wachters, J. Chem. Phys. **52**, 1033 (1970).
[19] P. J. Hay, J. Chem. Phys. **66**, 4377 (1977).
[20] K. Raghavachari and G. W. J. Trucks, J. Chem. Phys. **91**, 1062 (1989).
[21] M. J. Frisch, J. A. Pople, and J. S. Binkley, J. Chem. Phys. **80**, 3265 (1984).
[22] A. D. Becke, Phys. Rev. A **38**, 3098 (1988).
[23] C. Lee, W. Yang, and R. G. Parr, Phys. Rev. B **37**, 785 (1988).
[24] J. P. Perdew, Phys. Rev. B **33**, 8822 (1986).
[25] J. P. Perdew and Y. Wang, Phys. Rev. B **45**, 13244 (1992).
[26] J. P. Perdew, K. Burke, and M. Ernzerhof, Phys. Rev. Lett. **77**, 3865 (1996).
[27] A. D. Becke, J. Chem. Phys. **98**, 5648 (1993).
[28] P. J. Stevens, F. J. Devlin, C. F. Chablowski, and M. J. Frisch, J. Phys. Chem. **98**, 11623 (1994).
[29] G. L. Gutsev and C. W. Bauschlicher, Jr., J. Phys. Chem. A **105**, 10822 (2001).
[30] X. Li, H. Wu, X. B. Wang, and L. S. Wang, Phys. Rev. Lett. **81**, 1909 (1998).
[31] L. S. Wang and X. Li, in *Clusters and Nanostructure Interfaces*, edited by P. Jena, S. N. Khanna, and B. K. Rao (World Scientific, Singapore, 2000), pp. 293–300.
[32] J. Akola, M. Manninen, H. Hakkinen, U. Landman, X. Li, and L. S. Wang, Phys. Rev. B **60**, 11297 (1999).
[33] L. S. Wang, X. Li, and H. F. Zhang, Chem. Phys. **262**, 53 (2000).
[34] H. J. Zhai, L. S. Wang, A. N. Alexandrova, and A. I. Boldyrev, J. Chem. Phys. **117**, 7917 (2002).
[35] W. Grochala and R. Hoffmann, J. Phys. Chem. A **104**, 9740 (2000).
[36] S. Chrétien and D. R. Salahub, Phys. Rev. B **66**, 155425 (2002).
[37] K. P. Huber and G. Herzberg, *Constants of Diatomic Molecule* (Van Nostrand Reinhold, New York, 1979).
[38] P. Chen in *Unimolecular and Bimolecular Reactions Dynamics*, edited by C.-Y. Ng, T. Baer, and I. Powis (Wiley, Chichester, 1994) p. 371.
[39] K. M. Ervin, T. M. Ramond, G. E. Davico, R. L. Schwartz, S. M. Casey, and W. C. Lineberger, J. Phys. Chem. A **105**, 10822 (2001).
[40] P. C. Engelking and W. C. Lineberger, J. Chem. Phys. **66**, 5054 (1977).
[41] D. G. Leopold and W. C. Lineberger, J. Chem. Phys. **85**, 51 (1986).
[42] C. W. Bauschlicher, Jr. and G. L. Gutsev, Theor. Chem. Acc. **108**, 27 (2002).

Downloaded 25 Mar 2007 to 130.20.226.164. Redistribution subject to AIP license or copyright, see http://jcp.aip.org/jcp/copyright.jsp